Comparative analysis of opto-electronic performance of aluminium and silver nanoporous and nano-wired layers

Marus, Mikita; Hubarevich, Aliaksandr; Wang, Hong; Mukha, Yauhen; Smirnov, Aliaksandr; Huang, Hui; Sun, Xiao Wei; Fan, Weijun

2015

Marus, M., Hubarevich, A., Wang, H., Mukha, Y., Smirnov, A., Huang, H., et al. (2015). Comparative analysis of opto-electronic performance of aluminium and silver nano-porous and nano-wired layers. Optics Express, 23(20), 26794-26799.

https://hdl.handle.net/10356/81555

https://doi.org/10.1364/OE.23.026794

Comparative analysis of opto-electronic performance of aluminium and silver nanoporous and nano-wired layers

Mikita Marus,[1] Aliaksandr Hubarevich,[1] Hong Wang,[1] Yauhen Mukha,[2]Aliaksandr Smirnov,[2] Hui Huang[3], Xiao Wei Sun,[1,4] and Weijun Fan[1,*]

[1]School of Electrical and Electronic Engineering, Nanyang Technological University, 50 Nanyang Avenue, 639798, Singapore

[2]Department of Micro- and Nano-Electronics, Belarusian State University of Informatics and Radioelectronics, 6 P. Brovki, Minsk, 220013, Belarus

[3]Singapore Institute of Manufacturing Technology, 71 Nanyang Drive, Singapore 638075

[4]EXWSUN@ntu.edu.sg

**EWJFAN@ntu.edu.sg*

Abstract: The comparison of optical and electronic properties between randomly and uniformly arranged nano-wired layers of silver and aluminium was presented. The random configuration possessed similar average transmittance in the visible wavelength range, when the quantity of nano-wires was increased from 2 to 20 per area of 8×8 μm^2; and *higher* average transmittance up to 38% and 45% when the quantity of nano-wires was increased from 20 to 200 per area of 8×8 μm^2 for silver and aluminium nano-wired layers, respectively. Insignificant difference of the transmittance for silver and aluminium nano-wired layers was observed when the open area was less or equal to 55% regarding of the configuration. This difference became considerable as the open area grew larger than 55%: the uniform and random silver nano-wired possess up to 15% and 5% higher transmittance in comparison to aluminium nano-wired layers, respectively.

OCIS codes: (130.0250) Optoelectronics; (310.7005) Transparent conductive coatings; (240.6680) Surface plasmons.

References and links

1. S. Bae, S. J. Kim, D. Shin, J.-H. Ahn, and B. H. Hong, "Towards industrial applications of graphene electrodes," Phys. Scr. **2012**, 014024 (2012).
2. D. Zhang, K. Ryu, X. Liu, E. Polikarpov, J. Ly, M. E. Tompson, and C. Zhou, "Transparent, conductive, and flexible carbon nanotube films and their application in organic light-emitting diodes," Nano Lett. **6**, 1880-1886 (2006).
3. A. G. MacDiarmid, "Synthetic metals: a novel role for organic polymers," Synth. Met. **125**, 11-22 (2001).
4. G. Eda, G. Fanchini, and M. Chhowalla, "Large-area ultrathin films of reduced graphene oxide as a transparent and flexible electronic material," Nat. Nanotechnol **3**, 270-274 (2008).
5. K. S. Kim, Y. Zhao, H. Jang, S. Y. Lee, J. M. Kim, K. S. Kim, J.-H. Ahn, P. Kim, J.-Y. Choi, and B. H. Hong, "Large-scale pattern growth of graphene films for stretchable transparent electrodes," Nature **457**, 706-710 (2009).
6. N. Formica, P. Mantilla-Perez, D. S. Ghosh, D. Janner, T. L. Chen, M. Huang, S. Garner, J. Martorell, and V. Pruneri, "An Indium Tin Oxide-Free Polymer Solar Cell on Flexible Glass," ACS Appl. Mater. Interfaces **7**, 4541-4548 (2015).
7. M.-G. Kang, and L. J. Guo, "Metal transfer assisted nanolithography on rigid and flexible substrates," J. Vac. Sci. Technol. B **26**, 2421-2425 (2008).
8. P. B. Catrysse, and S. Fan, "Nanopatterned metallic films for use as transparent conductive electrodes in optoelectronic devices," Nano Lett. **10**, 2944-2949 (2010).
9. M. G. Kang, M. S. Kim, J. Kim, and L. J. Guo, "Organic solar cells using nanoimprinted transparent metal electrodes," Adv. Mater. **20**, 4408-4413 (2008).
10. M.-G. Kang, and L. J. Guo, "Semitransparent Cu electrode on a flexible substrate and its application in organic light emitting diodes," J. Vac. Sci. Technol. B **25**, 2637-2641 (2007).

11. J. van de Groep, P. Spinelli, and A. Polman, "Transparent conducting silver nanowire networks," Nano Lett. **12**, 3138-3144 (2012).
12. *NanoWeb: sub-micron transparent metal mesh conductors*. Available from: http://www.rolith.com/applications/transparent-conductive-electrodes.
13. L. Martin-Moreno, F. Garcia-Vidal, H. Lezec, K. Pellerin, T. Thio, J. Pendry, and T. Ebbesen, "Theory of extraordinary optical transmission through subwavelength hole arrays," Phys. Rev. Lett. **86**, 1114 (2001).
14. W.-D. Li, J. Hu, and S. Y. Chou, "Extraordinary light transmission through opaque thin metal film with subwavelength holes blocked by metal disks," Opt. Express **19**, 21098-21108 (2011).
15. T. W. Ebbesen, H. Lezec, H. Ghaemi, T. Thio, and P. Wolff, "Extraordinary optical transmission through sub-wavelength hole arrays," Nature **391**, 667-669 (1998).
16. J. Bhattacharya, N. Chakravarty, S. Pattnaik, W. D. Slafer, R. Biswas, and V. L. Dalal, "A photonic-plasmonic structure for enhancing light absorption in thin film solar cells," Appl. Phys. Lett. **99**, 131114 (2011).
17. K. Aydin, V. E. Ferry, R. M. Briggs, and H. A. Atwater, "Broadband polarization-independent resonant light absorption using ultrathin plasmonic super absorbers," Nat. Commun. **2**, 517 (2011).
18. A. Hubarevich, A. Kukhta, H. V. Demir, X. Sun, and H. Wang, "Ultra-thin broadband nanostructured insulator-metal-insulator-metal plasmonic light absorber," Opt. Express **23**, 9753-9761 (2015).
19. J.-Y. Lee, S. T. Connor, Y. Cui, and P. Peumans, "Solution-processed metal nanowire mesh transparent electrodes," Nano Lett. **8**, 689-692 (2008).
20. L. Hu, H. Wu, and Y. Cui, "Metal nanogrids, nanowires, and nanofibers for transparent electrodes," MRS Bull. **36**, 760-765 (2011).
21. B. Han, Y. Huang, R. Li, Q. Peng, J. Luo, K. Pei, A. Herczynski, K. Kempa, Z. Ren, and J. Gao, "Bio-inspired networks for optoelectronic applications," Nat. Commun. **5,** 5674 (2014).
22. D. Ghosh, L. Martinez, S. Giurgola, P. Vergani, and V. Pruneri, "Widely transparent electrodes based on ultrathin metals," Opt. Lett. **34**, 325-327 (2009).
23. M. Marus, A. Hubarevich, H. Wang, A. Smirnov, X. Sun, and W. Fan, "Optoelectronic performance optimization for transparent conductive layers based on randomly arranged silver nanorods," Opt. Express **23**, 6209-6214 (2015).
24. A. Hubarevich, M. Marus, W. Fan, A. Smirnov, X. W. Sun, and H. Wang, "Theoretical comparison of optical and electronic properties of uniformly and randomly arranged nano-porous ultra-thin layers," Opt. Express **23**, 17860-17865 (2015).
25. M. Jagota, and N. Tansu, "Conductivity of Nanowire Arrays under Random and Ordered Orientation Configurations," Sci. Rep. **5**, 10219 (2015).
26. *Lumerical FDTD Solutions*. Available from: https://www.lumerical.com/tcad-products/fdtd/.
27. B. Last, and D. Thouless, "Percolation theory and electrical conductivity," Phys. Rev. Lett. **27**, 1719 (1971).
28. J. Fitzpatrick, R. Malt, and F. Spaepen, "Percolation theory and the conductivity of random close packed mixtures of hard spheres," Phys. Lett. A **47**, 207-208 (1974).
29. S. Kirkpatrick, "Percolation and conduction," Rev. Mod. Phys. **45**, 574 (1973).
30. A. Hubarevich, M. Marus, A. Stsiapanau, A. Smirnov, J. Zhao, W. Fan, H. Wang, and X. Sun, "Transparent conductive nanoporous aluminium mesh prepared by electrochemical anodizing," Phys. Status Solidi A, accepted: early view (2015).
31. M. Marus, A. Hubarevich, H. Wang, A. Stsiapanau, A. Smirnov, X. W. Sun, and W. Fan, " Comparative analysis of opto-electronic performance of aluminium and silver nano-porous and nano-wired layers", submitted to Opt. Express, July 2015.
32. S. Xie, Z. Ouyang, B. Jia, and M. Gu, "Large-size, high-uniformity, random silver nanowire networks as transparent electrodes for crystalline silicon wafer solar cells," Opt. Express **21**, A355-A362 (2013).
33. M. Rycenga, C. M. Cobley, J. Zeng, W. Li, C. H. Moran, Q. Zhang, D. Qin, and Y. Xia, "Controlling the synthesis and assembly of silver nanostructures for plasmonic applications," Chem. Rev. **111**, 3669-3712 (2011).
34. D. Y. Choi, H. W. Kang, H. J. Sung, and S. S. Kim, "Annealing-free, flexible silver nanowire–polymer composite electrodes via a continuous two-step spray-coating method," Nanoscale **5**, 977-983 (2013).
35. H. H. Khaligh, and I. A. Goldthorpe, "Failure of silver nanowire transparent electrodes under current flow," Nanoscale Res. Lett. **8**, 1-6 (2013).
36. B. Huttner, "Optical properties of polyvalent metals in the solid and liquid state: aluminium," J. Phys.: Condens. Matter **6**, 2459 (1994).

1. Introduction

Transparent conductive layers (TCLs) are an essential component for majority of opto-electronic devices: liquid crystal, organic and quantum dot displays, solar cells, light emitting diodes, smart windows, touch screens and other applications [1-5]. The opto-electronic devices of new generation dictate advanced properties of TCLs such as flexibility, accessibility, ease of fabrication and low cost [6-10], which cannot be achieved with commonly used TCL based on indium-tin-oxide (ITO) due to inherent brittleness of the ITO ceramic films. Recent results demonstrate that nano-patterned metal TCLs may exceed the

opto-electronic performance of ITO, as well as possess the above mentioned properties [11, 12]. Another interesting features of metallic TCLs are related to surface plasmons at the interface between metal and dielectric at certain wavelengths, which can significantly tune their optical properties [13-18]. These facts demonstrate the attractiveness of the nano-patterned metallic TCL layers for the next wave of opto-electronic devices.

So far, the highest opto-electronic performance of the TCLs was obtained with uniformly arranged silver nanowire (NW) layers. The transmittance of 97% and the sheet resistance of 3 Ohm/sq was demonstrated by Rolith [12]. Interwire distance, wire diameter and thickness of the NW layer can be modified to obtain various application specific transmittance and sheet resistance [19-24]. Interesting results demonstrated in this year that randomly arranged NW layers can possess lower sheet resistance than uniformly arranged ones [23, 25]. However, it is still unclear whether uniformly or randomly arranged NW layers can have better transmittance. In this paper, the theoretical comparison of the optical and electronic properties between NW layers with uniform and random arrangement for silver (*Ag*) and aluminium (*Al*) is demonstrated. We show that *randomly* arranged NWs possess *similar* or *higher* average transmittance in visible wavelength range than uniform NW designs, which is depending on quantity of NWs per area.

2. Methodology

Figure 1 shows the geometrical models for uniformly and randomly arranged NW TCLs. The metal NWs were spread across the glass substrate within same plane which is parallel to *X* and *Y* axes. Cylindrical NWs of diameter *d* were uniformly arranged with interwire distance *a* [Fig. 1(a)], while random arranged NWs were distributed according to our previous work [23]: (i) initial position of NWs was set as in case of uniform arrangement; (ii) then each NW was arbitrarily shifted along *X* and *Y* axes for distance ranging from -1/5 to 1/5 of NW length; (iii) finally, each NW was arbitrarily tilted along *X* and *Y* axes for angle ranging from -90 to 90° [Fig. 1(b)]. The simulation area for the uniformly arranged NW layers was narrowed to the unit cell along *X* and *Y* axes, which side lengths are equal to the interwire distance *a*. In case of the randomly arranged NW layers, the unit cell was set to 8×8 μm^2 and simulated three times for arbitrarily position of the unit cell in order to justify the reproducibility of opto-electronic properties.

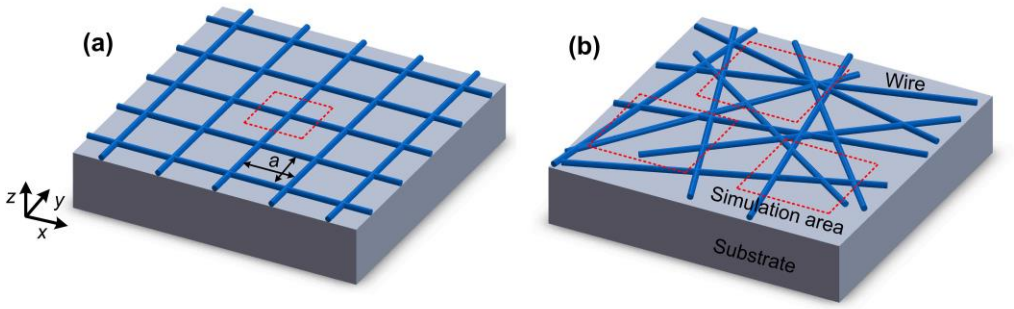

Fig. 1. Geometrical models of uniformly (a) and randomly (b) arranged NW layers on the glass substrate. Red rectangles are the unit simulation areas, which are equal to a^2 and 8×8 μm^2 for the NWs with uniform and random arrangement, respectively.

The optical properties were simulated using the finite-difference time-domain method (FDTD) which is commercially available within Lumerical software [26]. The incident light ranged from 300 to 900 nm was distributed along *Z* axis. The periodic boundary conditions and perfectly matched layers were applied parallel and perpendicular to *Z* axis correspondingly. Mesh size for metallic layers was set to 5, 5 and 2.5 nm in *X*, *Y*, and *Z*

directions, respectively. The sheet resistance is calculated by percolation model in accordance to [27-29], which is given by the following equation:

$$R_{sh} = \frac{1}{h\sigma_0 \left(\phi_f - \phi_{crit}\right)^t}, \tag{1}$$

where σ_0 is the conductivity of metal, ϕ_f is the volume fraction of patterned metal layer, ϕ_{crit} is the volume fraction threshold when the conductivity of patterned metal layer is zero, h is the thickness of the metal layer and t is the critical exponent. We assumed that both uniform and random NW layers have perfect contact of each crossing of NWs. Above mentioned methods were successfully applied by our group in [23, 24, 30, 31].

3. Results and discussion

The randomly arranged NWs of cylindrical shape with diameters of 30, 60 and 90 nm and length from 15 to 40 μm are typically implemented within experimental studies [32-35]. We set the diameter and length for both uniformly and randomly arranged NWs to 60 nm and 40 μm, respectively, while the quantity of NWs was varied from 2 to 200 per area of 8×8 μm^2. Figures 2(a) and 2(b) show the transmittance of *Ag* NW layers against the quantity of NWs with the uniform and random arrangement for the wavelength range from 300 to 900 nm. Dips of the transmittance in range from 300 to 450 nm are related to localized surface plasmons (LSPs) which are oscillations of electrons along the crosswise direction to the individual NWs [11]. Continuous decrement in the transmittance from 450-900 nm for NW layers with the uniform arrangement is attributed to surface plasmon polaritons (SPPs), which excite and propagate along the NWs [11]. The lower transmittance of the random NW layers in range from 450 to 550 nm can be explained by fewer amount of NWs rotated in the direction of electric field vector and thus exhibit less influence of SPPs on the transmittance.

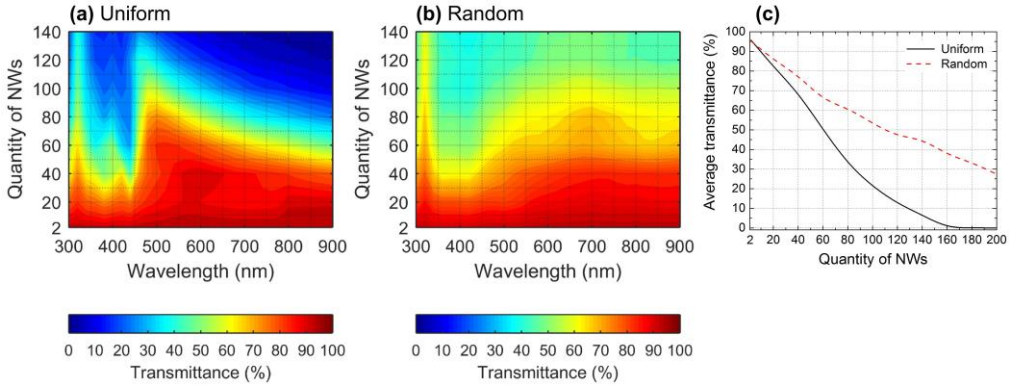

Fig. 2. Dependence of the transmittance of *Ag* NW layers on the quantity of NWs per area of 8×8 μm^2 with the uniform (a) and random (b) arrangement for the wavelength range from 300 to 900 nm. (c) Dependence of the average transmittance in visible spectrum on the quantity of NWs per area of 8×8 μm^2 for uniform and random arranged *Ag* NW layers.

Both the uniformly and randomly arranged NW layers possess similar transmittance, which is decreased from 97 to 85% when the quantity of NWs is increased from 2 to 20. Surprisingly, the difference of the transmittance between the uniform and random NW layers becomes significant when the quantity of NWs is increased from 20 to 200. *NW layers with random arrangement outperform uniform configuration* with up to 38% higher average transmittance in the visible spectrum as shown in Fig. 2(c). This behavior results from the

difference in distribution of the uniformly and randomly arranged NWs, which influence on open area. Figures 3(a) and 3(b) demonstrate the distribution of the uniform and random NWs with quantity of 140 per the simulation area. It is clearly seen that the open area is higher in case of the random configuration due to the stacking of the NWs. The difference of the open area between the uniform and random NW layers is increased from 0 to 24% with the increment of quantity of NWs from 20 to 200 as shown in Fig. 3(c).

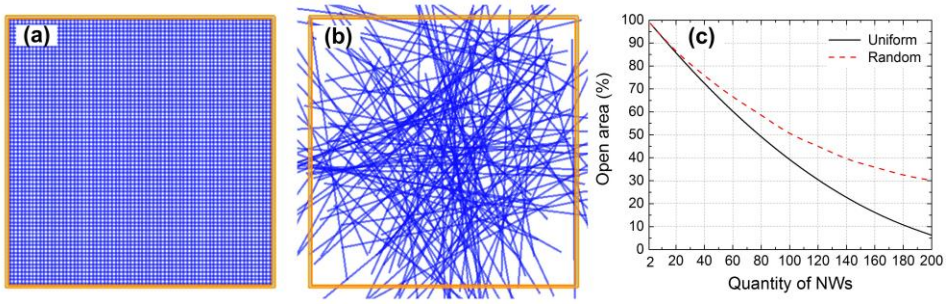

Fig. 3. The distribution of the uniform (a) and random (b) NWs for the quantity of 140 per 8×8 μm^2. (c) Dependence of the open area on the quantity of NWs per 8×8 μm2 for the uniform and random NW layers.

Figures 4(a) and 4(b) show the transmittance of *Al* NW layers against the quantity of NWs with the uniform and random arrangement for the wavelength range from 300 to 900 nm. Dips of transmittance for *Al* NW layers can be explained in the same manner as for *Ag* NW layers: (i) dips of the transmittance in range from 300 to 400 nm are related to localized surface plasmons (LSPs); (ii) continuous decrement in the transmittance from 450-900 nm for NW layers with the uniform arrangement is attributed to surface plasmon polaritons (SPPs). Another dip (iii) of the transmittance from 700 to 800 nm is due to interband electron transition in *Al* [36]. The transmittance of *Al* NW layers is higher in the range of 300 to 450 nm than the transmittance of *Ag* NW layers due to lower quality factor of LSPs in *Al* [33], which resulted in higher absorbance in *Ag*.

Similar trend as for *Ag* NW layers is observed when quantity of *Al* NWs is increased from 2 to 200: (i) both the uniformly and randomly arranged *Al* NW layers possess similar transmittance, which is decreased from 95 to 85% when the quantity of NWs is increased from 2 to 20; (ii) the difference of the transmittance between the uniform and random NW layers becomes significant when the quantity of NWs is increased from 20 to 200. *Al NW layers with random arrangement outperform uniform configuration* with up to 45% higher average transmittance in the visible spectrum as shown in Fig. 4(c). This fact is determined by same reason as for *Ag* NW layers, i.e. by the difference in distribution of the uniformly and randomly arranged NWs, which influence on open area [see Fig. 3(c)]. Insignificant difference of the average transmittance (less than 2%) between *Al* and *Ag* NW layers is observed when the open area is decreased from 100 till 55%. This tendency is changed when the open area is decreased below 55%: the transmittance of uniform and random *Al* NW layer in comparison with *Ag* NWs is less down to 15 and 5%, respectively. The larger difference of the average transmittance between the uniform configurations of *Al* and *Ag* NWs can be explained by the influence of SPPs on the transmittance: *Ag* possess higher quality factor of SPPs over whole simulation region [33]. In case of the random configurations of *Al* and *Ag* NW layers fewer amount of NWs is rotated in the direction of electric field vector, which results in less influence of SPPs on the transmittance.

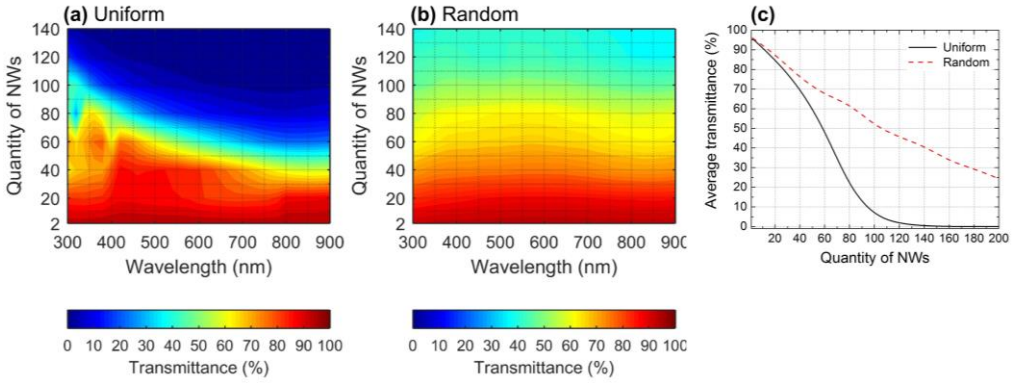

Fig. 4. Dependence of the transmittance of *Al* NW layers on the quantity of NWs per area of 8×8 μm^2 with the uniform (a) and random (b) arrangement for the wavelength range from 300 to 900 nm. (c) Dependence of the average transmittance in visible spectrum on the quantity of NWs per area of 8×8 μm^2 for uniform and random arranged *Al* NW layers.

Figure 5 illustrates the dependence of the sheet resistance on the average transmittance in visible wavelength spectrum for *Al* (left) and *Ag* (right) uniformly and randomly arranged NW layers. The difference of opto-electronic properties between uniform and random configurations keeps significant till the sheet resistance reaches 3 Ohm/sq, when the quantity of NW decreases from 200 to 20. The transmittance of *Ag* NW layers at the sheet resistance of 0.65 Ohm/sq is equal to 30 and 70% for uniform and random arrangement, respectively. At the sheet resistance of 3 Ohm/sq, the transmittance of *Ag* NW layers is 79 and 84% for uniform and random arrangement, respectively. Thus, the difference of the transmittance decreased from 40 to 5% between above mentioned configurations of *Ag* NWs. In case of *Al* NW layers this difference is decreased from 38 to 4%, when the sheet resistance increased from 1.25 to 3 Ohm/sq. As the sheet resistance grows further with the decrement of quantity of NWs, the difference of the transmittance between uniform and random NW layers consequently decreases from 5% down to negligible value, when quantity of NWs is equal to 2. The sheet resistance of both uniform and random *Ag* NW layers is lower than *Al* NW layers due to higher bulk conductivity σ_0 of *Ag*: 6.3×10^7 S/m versus 3.5×10^7 S/m for *Al*.

Thus, randomly arranged metallic NW layers are more promising for the applications demanding lowest sheet resistance such as solar cell and displays, while the influence of configuration of NWs becomes insignificant for the applications requiring higher sheet resistance such as touch screens and smart windows.

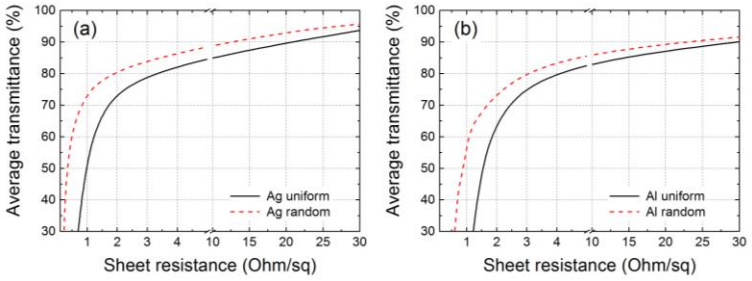

Fig. 5. Sheet resistance versus average transmittance in visible wavelength spectrum for *Al* (left) and *Ag* (right) uniformly and randomly arranged NWs layers.

4. Conclusion

The comparative analysis of optical and electronic properties of randomly and uniformly arranged NW layers of *Ag* and *Al* was presented. It was found, that the random configuration possessed similar average transmittance in the visible wavelength range, when the quantity of NWs was increased from 2 to 20 per area of 8×8 μm^2; and *higher* average transmittance up to 38% and 45% when the quantity of NWs was increased from 20 to 200 per area of 8×8 μm^2 for *Ag* and *Al* NW layers, respectively. Insignificant difference of the transmittance for *Ag* and *Al* NW was observed when the open area was less or equal to 55% regarding of the configuration. It became considerable as the open area grew larger than 55%: the uniform and random *Ag* NW possess up to 15% and 5% higher transmittance, respectively, in comparison to *Al* NW layers. Therefore, randomly arranged metallic NW layers are more promising for the applications demanding lowest sheet resistance such as solar cell and displays, while the influence of configuration of NWs becomes insignificant for the applications requiring higher sheet resistance such as touch screens and smart windows.

Acknowledgment

This project is supported by National Research Foundation of Singapore (No. NRF-CRP11-2012-01).